Am J Physiol Heart Circ Physiol 283: H372–H381, 2002;
10.1152/ajpheart.01091.2001.

Correlation of repolarization of ventricular monophasic action potential with ECG in the murine heart

STEPHAN DANIK,[1] CANDIDO CABO,[2,3] CHRISTINE CHIELLO,[2] SACHA KANG,[2] ANDREW L. WIT,[2,3] AND JAMES COROMILAS[1]

Departments of [1]Medicine, and [2]Pharmacology, and [3]The Center for Molecular Therapeutics, College of Physicians and Surgeons of Columbia University, New York, New York 10032

Received 11 December 2001; accepted in final form 1 March 2002

Danik, Stephan, Candido Cabo, Christine Chiello, Sacha Kang, Andrew L. Wit, and James Coromilas. Correlation of repolarization of ventricular monophasic action potential with ECG in the murine heart. *Am J Physiol Heart Circ Physiol* 283: H372–H381, 2002;10.1152/ajpheart.01091.2001.—Transgenic mice have become important experimental models in the investigation of mechanisms causing cardiac arrhythmias because of the ability to create strains with alterations in repolarizing membrane currents. It is important to relate alterations in membrane currents in cells to their phenotypic expression on the electrocardiogram (ECG). The murine ECG, however, has unusual characteristics that make interpretation of the phenotypic expression of changes in ventricular repolarization uncertain. The major deflection representing the QRS (referred to as "*a*") is often followed by a secondary slower deflection ("*b*") and sometimes a subtle third deflection ("*c*"). To determine whether the second or third deflections or both represent ventricular repolarization, we recorded the ventricular monophasic action potential (MAP) in open-chest mice and correlated repolarization with the ECG. There was no significant correlation by linear regression, between action potential duration to 50% or 90% repolarization (APD_{50} or APD_{90}), respectively, of the MAP and either the interval from onset of Q to onset of *b* (Qb interval) or onset of *c* (Qc interval). Administration of 4-aminopyridine (4-AP) significantly prolonged APD_{50} and APD_{90} and the Qb interval, indicating that this deflection on the ECG represents part of ventricular repolarization. After 4-AP, the *c* wave disappeared, also suggesting that it represents a component of ventricular repolarization. Although it appears that both the *b* and *c* waves that follow the Q wave on the ECG represent ventricular repolarization, neither correlates exactly with APD_{90} of the MAP. Therefore, an accurate measurement of complete repolarization of the murine ventricle cannot be obtained from the surface ECG.

arrhythmias

TRANSGENIC MICE HAVE BECOME important experimental models in the investigation of mechanisms causing cardiac arrhythmias because of the ability to create strains with alterations in cardiac ion channel function. Of particular interest has been the creation of transgenic models of the long QT syndrome (LQTS), in which changes in ventricular repolarization have been induced by altering ion channels contributing to phases 2 and 3 of the action potential (2, 4, 5, 9, 32, 48). In such studies, in which ion channel function has been altered, it is important to evaluate the phenotypic expression on the electrocardiogram (ECG) to document that the electrical activity of the heart, as well as its cells, is changed in the desired way. The murine ECG, however, has some unusual characteristics that make interpretation of the phenotypic expression of changes in ventricular repolarization uncertain. The major deflection (*a*) representing the QRS (Fig. 1) is often followed by a secondary slower deflection (*b*) (Fig. 1). Sometimes a subtle third positive or negative wave (*c*) follows (Fig. 1). It is not clear which of the second and third deflections (*b* and *c* in Fig. 1) represents ventricular repolarization with some investigators designating *b* as the T wave (20, 23, 25, 26, 48) and others *c* (4, 5, 7, 23, 28, 32, 33).

To analyze the murine ECG with respect to the identification of ventricular repolarization, we recorded the ventricular monophasic action potential (MAP) from the in situ murine heart and correlated its time course with the waveforms on the ECG.

METHODS

Murine preparation for ECG measurements. Studies were performed on Swiss Webster mice aged 6–12 wk, weighing 31–41 g, that were anesthetized with pentobarbital sodium (0.033 mg/g ip). A 20-gauge polyethylene catheter was inserted into the trachea that was exposed in the neck. The mouse was then mechanically ventilated with positive pressure at 170 breaths/min with a tidal volume of 0.5 ml (model 687, Harvard Apparatus). A rectal probe was used to measure body temperature that was maintained within a range of 35–38°C with a heating lamp. A catheter was placed in the internal jugular vein for the administration of drugs.

A standard 12-lead ECG was obtained by placement of subcutaneous 22-gauge needles in each limb and rotating a chest lead to the standard locations of the precordial leads. ECGs were recorded on a VR 12 Recorder (Electronics for Medicine; Pleasantville, NY). All data were digitized and analyzed on a Windaq Waveform Browser (DATAQ Instruments; Akron, OH).

Address for reprint requests and other correspondence: J. Coromilas, Dept. of Medicine, College of Physicians and Surgeons of Columbia University, 630 W. 168th St., New York, NY 10032.

The costs of publication of this article were defrayed in part by the payment of page charges. The article must therefore be hereby marked "*advertisement*" in accordance with 18 U.S.C. Section 1734 solely to indicate this fact.

 0363-6135/02 $5.00 Copyright © 2002 the American Physiological Society

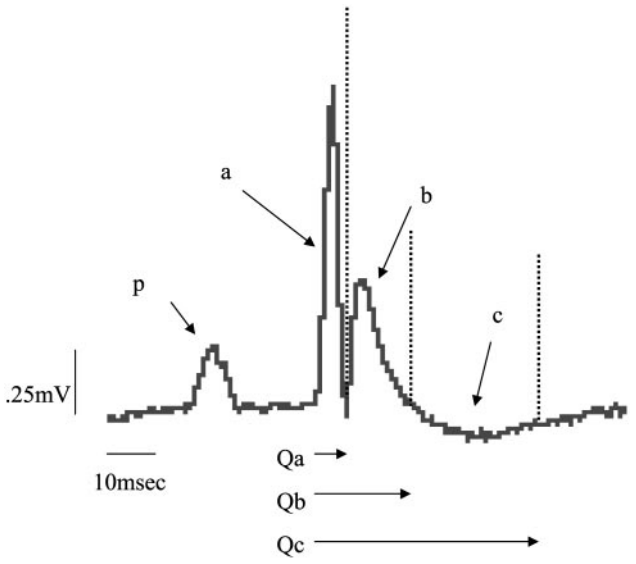

Fig. 1. Illustration of one heartbeat on the murine electrocardiogram (ECG). After the P wave, there is a major positive deflection designated as *a*. It is followed by a second slower positive deflection *b* and a subtle negative wave *c*. Arrows at bottom of figure designate the Qa, Qb, and Qc intervals, measured from the onset of the Q to the vertical lines.

After the 12-lead ECG had been obtained during sinus rhythm, a midline sternotomy (a 2- to 3-cm incision) was performed with the use of fine scissors. Each chest flap was pulled back with a suture that was tied to a post. The pericardium was peeled back with fine forceps to expose the heart. After the chest was opened, only six leads of the ECG were recorded (I-III, aVR, aVL, and aVF) because precordial ECGs could not be obtained.

MAP recording. MAPs were recorded from the anterior surface of the left ventricle using a modified Franz MAP electrode (15) constructed from teflon-coated silver wires. The tip of the wire in contact with the heart had a diameter of 0.25 mm, a size shown to accurately record the time course of repolarization in the murine heart (27). The recording electrode was positioned in the center of a polyethylene tube (1 mm diameter). The ground electrode was fastened to the outside of the tube several millimeters above the tip. The polyethylene tubing was then positioned on the heart so that the central silver wire made contact with the ventricular surface, whereas the ground electrode was above the surface. Gentle suction was sometimes applied through the tubing to stabilize the recording. However, the MAP was obtained when the central silver wire made contact with the heart and mild pressure was applied; it was not dependent on the application of suction. Both recording and ground electrodes were connected to a DC-coupled preamplifier (model 111101, EP Technologies; Mountain View, CA). A MAP was obtained in each animal during sinus rhythm while six leads of the ECG were simultaneously recorded. A MAP was considered stable if the sequence of depolarization and repolarization was uniform in amplitude and shape throughout the experiment (typically lasting 30–60 min) with a relatively constant baseline (some baseline movement was accepted) without the need for manual manipulation of the electrode contact.

Programmed stimulation of the ventricles was accomplished through a bipolar stimulating electrode positioned on the apex of the left ventricle, to measure the ventricular effective refractory period (VERP) while MAP was recorded. The ventricles were paced at a basic cycle length of 100 ms and single premature stimuli were decremented by 5 ms to a coupling interval of 55 ms and then by 2-ms intervals. Stimuli were two times diastolic threshold and 2 ms duration. The VERP was defined as the longest coupling interval of a premature stimulus that did not elicit a propagated response as seen on the ECG. For each animal, at least three pacing trials were done with the VERP the average of the trials.

In eight experiments, 4-aminopyridine (4-AP) (aliquots of 0.05 ml of 0.0625 M solution) was administered into the external jugular vein to block the transient outward potassium current (I_{to}), a major contributor to repolarization of the murine ventricular action potential (11, 17, 18, 45, 46, 49). The atria were stimulated at a cycle length of 100 ms to control the heart rate during drug administration and the MAP and ECG intervals measured. VERP was also determined as described above.

Data analysis. Measurements were obtained from the ECG before opening the chest. The sinus cycle length (R-R interval) and PQ interval (onset of the P wave to the beginning of the QRS complex) were determined. The deflections occurring after the P wave were divided into three segments as illustrated in Fig. 1. The interval from the beginning of the QRS complex where it first deviated from the isoelectric line to the end of the first major deflection (*a*) was designated as Qa. As shown in Fig. 1, the terminal component of the positive *a* wave in the murine ECG sometimes does not reach the isoelectric line because its return is interrupted by a second slower and lower amplitude-positive deflection (*b* wave). The change in slope from negative to positive signified the end of the *a* deflection and the onset of the *b* deflection. Otherwise, the *a* wave terminates in a negative wave (Fig. 2, leads V2–6) that returns to the isoelectric line where the *a*

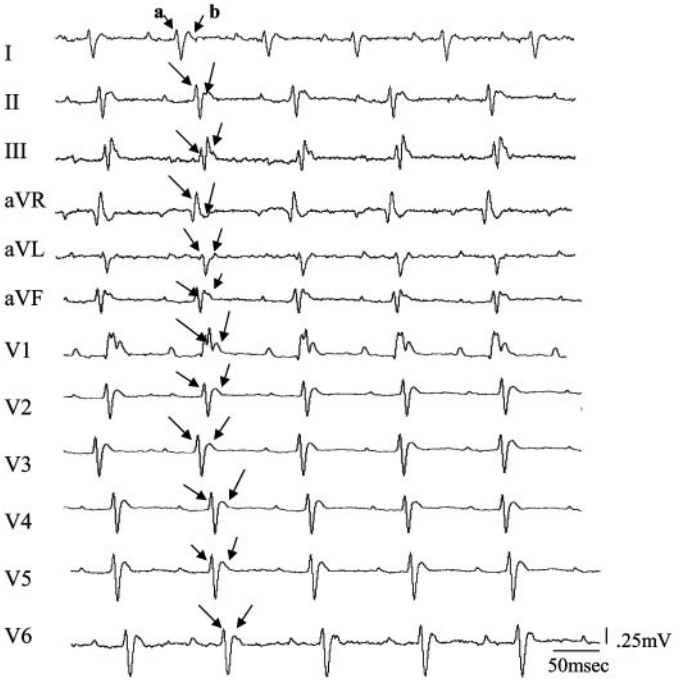

Fig. 2. Example of a 12-lead ECG of a closed-chest anesthetized mouse (#8). The *a* and *b* deflections are indicated by arrows but a *c* wave cannot be identified in any of the 12 leads. The sinus cycle length (SCL) is 109 ± 1 ms. Leads were recorded sequentially so deflections are not aligned.

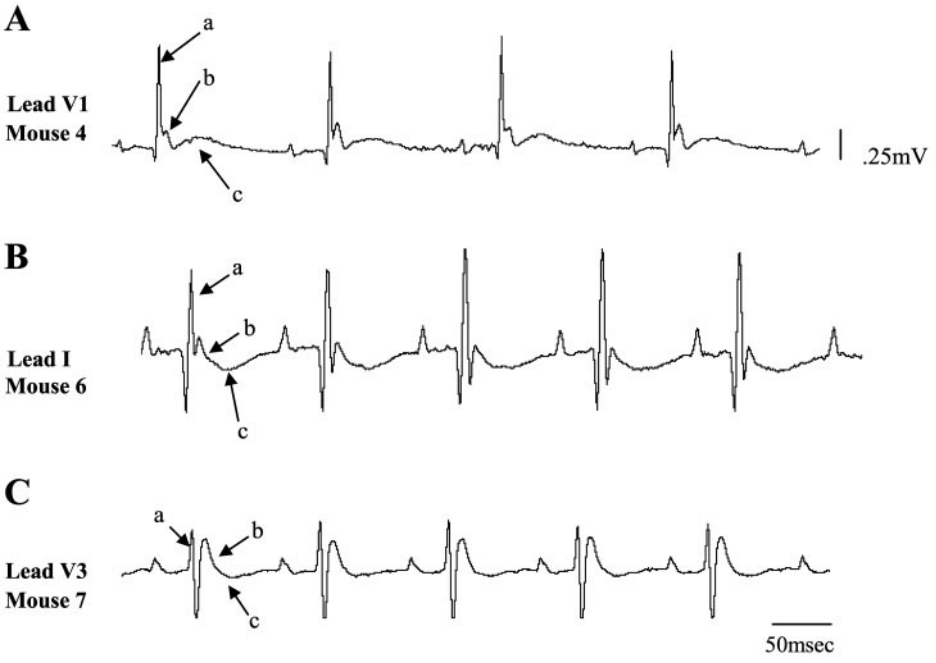

Fig. 3. *A-C*: ECG leads showing *a*, *b*, and *c* waves that were recorded in three different anesthetized mice.

wave ends. It is then followed by a slower positive *b* wave. The time of onset from the beginning of the QRS complex to the end of this second *b* deflection, at the point that it returns to the isoelectric line, was designated as the Qb interval. After the *b* deflection, a slow negative or positive wave sometimes occurs (*c* wave in Fig. 1). The time of onset from the beginning of the QRS complex to the end of deflection *c* is reported as the Qc interval. Measurements of these intervals were made for at least six beats for each of the 12 leads in each experiment and the mean values (±SD) calculated. The measurements were repeated after the chest was opened, from the six ECG leads that could still be recorded.

The intervals measured on the surface ECG were compared with the time course of repolarization obtained from the MAPs during sinus rhythm. The MAP duration to 50% repolarization (APD_{50}) was measured from the fastest part of the MAP upstroke to 50% repolarization, determined as 50% of the distance between the crest of the MAP "plateau" phase (maximum level of depolarization after termination of the upstroke) and the diastolic baseline (see Fig. 13 in Ref. 15). The APD_{90} duration was measured from the same point on the upstroke to 90% repolarization from the crest of the plateau phase to the diastolic baseline (15). The mean of six randomly selected APD_{50} and APD_{90} values was calculated and compared with mean values of ECG waveforms on each lead in each animal. Because sinus cycle length did not vary significantly under different conditions in which the ECG and APD were measured and compared (see RESULTS), corrections for changes in cycle length were not necessary. The APD_{50} and APD_{90} were also determined during programmed stimulation of the ventricles at a basic cycle length of 100 ms. The mean value of eight randomly selected APD_{50} and APD_{90} during pacing was calculated.

Values for Qa, Qb, and Qc intervals in the closed-chest mouse were compared with the respective values after the chest was opened. This was done by plotting the values in

Table 1. *ECG intervals of closed-chest mice*

		Qa		Qb		Qc	
Experiment	SCL	Interval	Leads	Interval	Leads	Interval	Leads
1	106 ± 4	10 ± 1	12/12	21 ± 1	12/12	ND	
2	162 ± 7	8 ± 1	12/12	20 ± 1	12/12	ND	
3	129 ± 3	9 ± 1	12/12	20 ± 2	12/12	ND	
4	142 ± 7	9 ± 1	12/12	24 ± 3	12/12	74 ± 6	1(V1)
5	151 ± 2	10 ± 2	12/12	23 ± 3	12/12	ND	
6	111 ± 1	10 ± 1	12/12	24 ± 2	12/12	70 ± 1	3 (I, aVR, aVL)
7	107 ± 4	9 ± 1	12/12	24 ± 3	12/12	59 ± 4	5(V3)
8	109 ± 1	11 ± 3	12/12	26 ± 2	12/12	ND	
9	104 ± 6	8 ± 0	12/12	23 ± 3	11/12	63 ± 0	1(V1)
10	103 ± 1	8 ± 1	12/12	20 ± 1	11/12	ND	
11	139 ± 4	8 ± 3	12/12	18 ± 3	11/12	ND	
12	106 ± 5	8 ± 1	12/12	21 ± 1	11/12	ND	
13	103 ± 2	8 ± 1	12/12	20 ± 2	12/12	59 ± 4	1(aVL)
Means ± SE	121 ± 21	9 ± 1		22 ± 2		65 ± 7	

ECG, electrocardiogram; SCL, sinus cycle length; ND, not determined. Interval is defined in METHODS as measured in milliseconds. Leads refer to the number of leads in which deflection was recorded and total number of leads recorded for Qc. Leads in which the *c* wave was recorded are indicated in parentheses.

Table 2. *ECG intervals of open-chest mice*

		Qa		Qb		Qc	
Experiment	SCL	Interval	Leads	Interval	Leads	Interval	Leads
1	96 ± 3	10 ± 2	6/6	21 ± 1	6/6	50 ± 2	1 (II)
2	124 ± 2	9 ± 1	6/6	23 ± 1	6/6	57 ± 9	6 (I–III, aVR, aVL)
3	120 ± 1	9 ± 1	6/6	21 ± 1	6/6	ND	
4	113 ± 1	9 ± 1	6/6	23 ± 1	6/6	ND	
5	107 ± 2	11 ± 3	6/6	23 ± 1	5/6	ND	
6	112 ± 1	10 ± 1	6/6	23 ± 2	6/6	56 ± 1	4 (I, II, aVR, aVL)
7	113 ± 2	9 ± 1	6/6	24 ± 2	6/6	ND	
8	108 ± 1	11 ± 2	6/6	24 ± 2	6/6	ND	
9	104 ± 1	8 ± 0	6/6	22 ± 2	5/6	ND	
10	115 ± 1	8 ± 0	6/6	20 ± 1	6/6	73 ± 1	1 (III)
11	106 ± 1	8 ± 1	6/6	20 ± 1	5/6	ND	
12	102 ± 1	8 ± 1	6/6	19 ± 2	6/6	54 ± 2	3 (I, aVR, aVL)
13	109 ± 6	8 ± 1	6/6	21 ± 1	5/6	ND	
Means ± SE	110 ± 7	9 ± 1		22 ± 2		58 ± 9	

each of the respective six limb leads in the closed-chest mouse against the open-chest mouse; correlation was determined by linear regression analysis using SyStat and SigmaPlot software. Repolarization measurements determined from the MAP were correlated with the surface ECG measurements obtained with the chest both closed and opened. Values of the Qa, Qb, and Qc intervals were plotted against the APD_{50} and APD_{90} and the correlation determined by linear regression analysis.

RESULTS

Murine ECG characteristics: closed- and open-chest comparisons. Figure 2 illustrates a 12-lead ECG recorded from a closed-chest anesthetized mouse in sinus rhythm. The *a* and *b* deflections are present in all leads (arrows) but the *c* deflection is not identifiable in any of the leads. A clearly defined Qc was seen in only 5 of 13 mice and not in all leads (Fig. 3). Measured values and frequency of occurrence of ECG intervals are presented in Table 1.

Table 2 summarizes the ECG intervals of the same 13 mice after the chest was opened. The sinus cycle length and the Qa and Qb intervals (which were recorded in all leads) were not significantly different from the values determined with the chest closed ($P > 0.5$). A *c* deflection was recorded in five mice, four in which no *c* was recorded before the chest was opened (nos. 1, 2, 10, 12). A *c* wave was not recorded in four of five mice in which it was seen before the chest was opened (nos. 4, 7, 9, 13). The Qc interval after the chest was open was not significantly different ($P = 0.20$) than before the chest was open, although it was measured mostly in different mice (Table 2).

After the MAP electrode was placed on the mouse heart, the mean sinus cycle length was not changed significantly ($P = 0.33$). The Qa and Qb intervals were also unchanged ($P > 0.5$) (Table 3). There was a high degree of correlation for Qa ($r^2 = 0.73$, $P < 0.001$) and Qb ($r^2 = 0.68$, $P < 0.001$) before and after the chest was open and when the electrode was placed on the heart for each experiment. After the MAP electrode was placed on the heart, a *c* wave was recorded in seven experiments, in 15 of 42 leads (Table 3). The mean Qc interval was not different from the mean Qc before the MAP electrode was in place ($P = 0.59$).

MAP and VERP measurements. A stable MAP was recorded in each experiment. MAP amplitudes ranged from 3.3 to 15.1 mV (mean 7.7 ± 5.1 mV). An example is shown in Fig. 4. MAPs were characterized by a rapid

Table 3. *ECG intervals of open-chest mice with MAP*

		Qa		Qb		Qc	
Experiment	SCL	Interval	Leads	Interval	Leads	Interval	Leads
1	101 ± 1	11 ± 1	6/6	22 ± 1	6/6	59 ± 2	1 (aVF)
2	126 ± 1	9 ± 1	6/6	24 ± 2	6/6	55 ± 8	3 (I, III, aVF)
3	107 ± 1	9 ± 1	6/6	21 ± 3	6/6	ND	
4	135 ± 1	9 ± 1	6/6	24 ± 3	6/6	ND	
5	106 ± 1	11 ± 3	6/6	24 ± 3	6/6	ND	
6	119 ± 1	10 ± 1	6/6	24 ± 2	6/6	ND	
7	96 ± 1	8 ± 1	6/6	22 ± 3	6/6	54 ± 2	1 (aVL)
8	113 ± 1	12 ± 1	6/6	25 ± 1	5/6	46 ± 3	1 (I)
9	110 ± 3	8 ± 0	6/6	21 ± 4	6/6	64 ± 3	5 (I, II, III, aVL, aVF)
10	115 ± 1	8 ± 1	6/6	22 ± 2	6/6	54 ± 2	3 (I, III, aVL)
11	106 ± 0	8 ± 1	6/6	20 ± 1	5/6	58 ± 3	1 (III)
12	106 ± 1	8 ± 0	6/6	20 ± 2	6/6	ND	
13	127 ± 1	8 ± 1	6/6	22 ± 1	5/6	ND	
Means ± SE	112 ± 12	9 ± 1		22 ± 1		52 ± 5	

MAP, monophasic action potential.

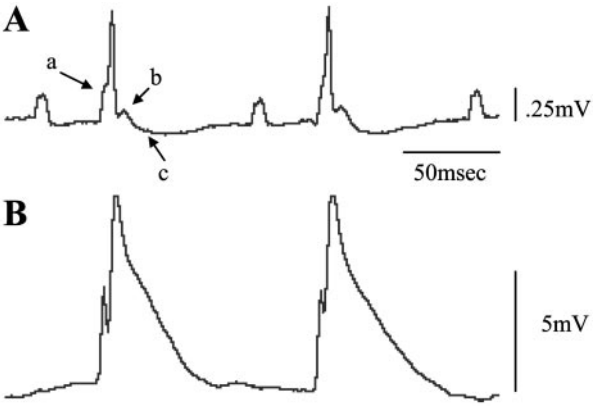

Fig. 4. Monophasic action potential (MAP) and lead II ECG recording in one experiment. SCL is 126 ± 1 ms. Action potential duration to 50% repolarization (APD_{50}) is 21 ± 1 and APD to 90% repolarization (APD_{90}) is 63 ± 1 ms.

depolarization spike (*phase 0*) and an initial rapid phase of repolarization (*phase 1*) that merged with a terminal repolarization phase (3) with little or no plateau phase (2). The summary data for the time course of MAP repolarization during sinus rhythm and during ventricular pacing at a basic cycle length of 100 ms are presented in Table 4.

Figure 5 shows MAP and ECG recordings during measurement of the VERP. The VERP was less than the APD_{90} in each experiment (Table 4). There is a high degree of correlation between the APD_{90} measured on the MAP and the VERP (Fig. 5, *inset*; $r^2 = 0.68$, $P < 0.001$).

Comparison of repolarization of MAP with ECG. The mean Qb interval with the chest open and the MAP electrode in place was 22 ± 1 ms (Table 3), whereas the mean APD_{90} was 53 ± 6 ms, and APD_{50} was 21 ± 6 (Table 4). An analysis of linear regression comparing Qb with APD_{90} ($r^2 = 0.144$, $P = 0.20$) and APD_{50} ($r^2 = 0.0073$, $P = 0.782$) showed no significant correlation (Fig. 6). In addition, an analysis of linear regression was done by comparing Qb in each lead in each mouse for the three conditions during which ECGs were recorded (closed chest, open chest, and open chest with MAP electrode on the heart) with the corresponding APD_{50} and APD_{90} of MAPs recorded in each experiment. No significant correlation was found between any lead and either measure of repolarization.

The mean Qc interval with the MAP in place (52 ± 5; Table 3) was not significantly different from the APD_{90} (53 ± 6; Table 4; $P = 0.33$). Figure 7*A* shows no correlation by linear regression between APD_{90} and Qc ($r^2 = 0.14$, $P = 0.41$), and the relationship is significantly different from the line of identity along which APD_{90} and Qc would be equal. Similarly, there is no correlation between APD_{50} and the Qc interval ($r^2 = 0.35$, $P = 0.162$) (Fig. 7*B*).

Effects of 4-AP on MAP and ECG. 4-AP significantly prolonged MAP APD_{50} (from 16 ± 3 to 28 ± 4 ms) ($P < 0.0007$) and APD_{90} (from 48 ± 4 to 60 ± 4 ms) ($P < 0.0008$) when the heart rate was controlled by atrial pacing (Fig. 8 and Table 5). The VERP, determined during ventricular pacing, was prolonged (from 32 ± 4 to 56 ± 4 ms) ($P < 0.0001$) (Table 5). 4-AP did not change the Qa interval (9 ± 2 ms both before and after 4-AP). However, the Qb interval was significantly lengthened from 23 ± 3 to 36 ± 6 ms ($P < 0.003$) (Table 5 and Fig. 8). We were not able to determine the effects of 4-AP on the Qc interval during atrial pacing because at the pacing cycle lengths at which the heart could be captured, much of the *c* wave, when it occurred, was obscured by the next atrial paced beat. Therefore, the effect of 4-AP on the Qc was determined during sinus rhythm in the three experiments in which it was present during control. In these experiments, 4-AP lengthened the sinus cycle length (Table 5) from 111 ± 5 ms to 125 ± 6 ms ($P = 0.14$). As in the experiments with atrial pacing, Qb ($P < 0.05$), APD_{50} ($P < 0.02$), and APD_{90} ($P < 0.04$) were significantly lengthened by 4-AP. In all experiments, the *c* wave disappeared after 4-AP, so no measurements of its change in duration could be obtained (Fig. 9).

DISCUSSION

Where is the T wave on murine ECG? In studies (39) on the LQTS, correlations have been made in human subjects among genetically determined alterations in

Table 4. *MAP and VERP*

Experiment	SCL	APD_{50}	APD_{90}	APD_{50P}	APD_{90P}	VERP
1	101 ± 1	33 ± 1	59 ± 1	39 ± 2	59 ± 4	37 ± 6
2	126 ± 1	21 ± 1	63 ± 1	16 ± 1	58 ± 3	38 ± 3
3	107 ± 1	20 ± 2	57 ± 1	19 ± 2	59 ± 2	38 ± 0
4	135 ± 1	19 ± 1	57 ± 1	18 ± 1	47 ± 4	32 ± 1
5	106 ± 1	23 ± 1	55 ± 1	18 ± 1	57 ± 4	42 ± 0
6	119 ± 1	17 ± 1	54 ± 1	24 ± 2	53 ± 2	36 ± 0
7	96 ± 1	18 ± 1	48 ± 1	19 ± 2	48 ± 1	32 ± 0
8	113 ± 1	19 ± 2	49 ± 2	23 ± 1	50 ± 1	33 ± 1
9	110 ± 3	31 ± 1	58 ± 1	32 ± 2	59 ± 2	37 ± 1
10	115 ± 1	17 ± 3	49 ± 3	21 ± 1	48 ± 1	29 ± 1
11	106 ± 0	15 ± 1	44 ± 1	19 ± 1	50 ± 1	29 ± 2
12	106 ± 1	20 ± 2	47 ± 1	25 ± 1	50 ± 1	28 ± 0
13	127 ± 1	20 ± 2	50 ± 1	24 ± 1	50 ± 1	29 ± 1
Means ± SE	113 ± 11	21 ± 6	53 ± 6	22 ± 7	54 ± 5	36 ± 4

VERP, ventricular effective refractory period; APD_{50} and APD_{90}, action potential duration to 50% and 90% repolarization, respectively; APD_{50p} and APD_{90p} were obtained during ventricular pacing at 100-ms cycle length.

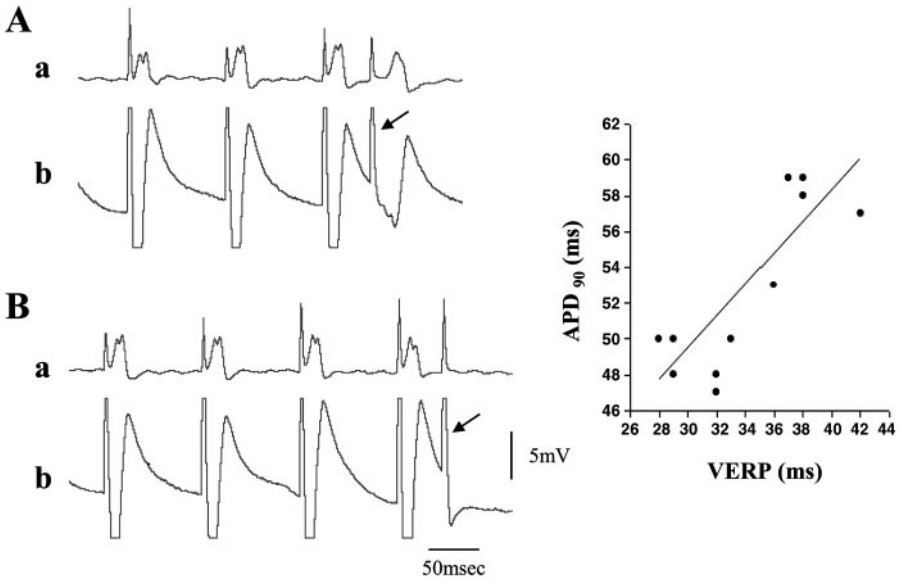

Fig. 5. MAP and ECG recordings during determination of the ventricular effective refractory period (VERP). *A*: following 12 paced beats (S_1) at a CL of 100 ms, an S_2 (arrow) after 40 ms elicits a propagated response. *B*: at a slightly shorter coupling interval of 35 ms, there is no response to S_2 (arrow). *Inset*: VERP is significantly correlated with APD_{90} ($r^2 = 0.68$, $P < 0.001$).

cardiac ion channel function, the appearance of an abnormal ECG, and the occurrence of life-threatening ventricular arrhythmias. Another approach to understanding the pathophysiology of long QT has been the use of transgenic mice, in which alterations have been made in specific genes controlling ion channels that govern repolarization (2, 4, 5, 9, 32, 48). To understand the pathophysiological significance of such genetic changes, it is important to determine their impact not only at the cellular level but also on the whole heart, i.e., on ECG indicators of repolarization. The ability to show a change in the T wave and QT interval in the mouse with genetically altered ion channels assumes that these markers of repolarization are readily identifiable. An examination of the murine ECG, however, shows differences from that of larger mammals, particularly the absence of a well-defined T wave separated from the QRS by an ST segment. This was recognized as early as 1929 by Agduhr and Stenstrom (1), who stated that ". . . T summits can almost never be discovered (in the murine heart), which seems noteworthy, in as much as other inflections are sometimes nearly as large as those of the human ECG. Instead of an independent T summit, there appears, however, with great consistency, terminating the QRS complex, a slow diphasic shape. . .." This "diphasic" shape describes what we have designated as the *a* and *b* waves in Fig. 1. They concluded that the notch at the end of the major deflection (*b* wave) was the T wave, a conclusion ascribed to in subsequent reports on mice (30, 31, 37, 38), shrews (34, 44), and rats (40). In more recent studies on transgenic models of LQTS, a third slow wave (the *c* wave in Fig. 1) has sometimes been identified as the T wave (4, 5, 7, 23, 28, 32, 33). The QT interval has been considered to be a return to the isoelectric baseline, whether this occurs from the *b* wave (Qb interval) or from the *c* wave if present (Qc interval). Such variations in measurements may have led to the wide range of reported QT values, from 27 to 109 ms (2, 4–7, 16, 21, 23, 28, 29, 32, 33, 48). Uncertainty in the exact identification of the T wave may also have sometimes led to conclusions that the surface

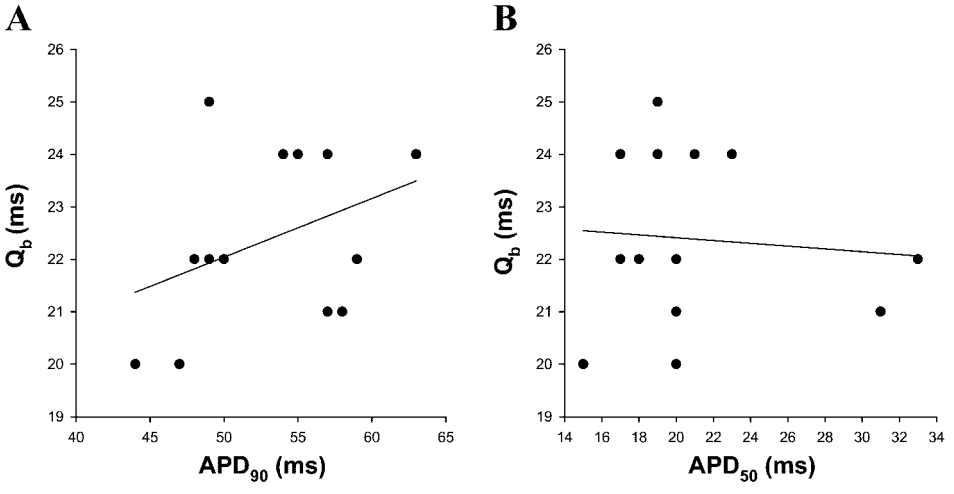

Fig. 6. *A*: correlation between the Qb interval (ordinate) and APD_{90} of the MAP ($r^2 = 0.144$, $P = 0.20$). *B*: correlation between the Qb interval (ordinate) and APD_{50} of the MAP ($r^2 = 0.0073$, $P < 0.782$).

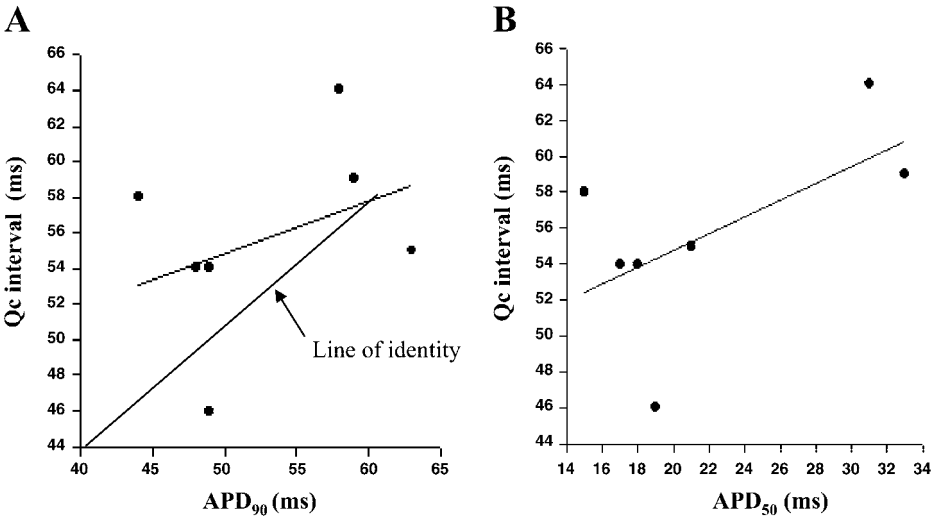

Fig. 7. *A*: correlation between APD_{90} and the Qc interval ($r^2 = 0.14$, $P = 0.41$) in the open-chest mouse during sinus rhythm. *B*: correlation between the Qc interval and APD_{50} in the open-chest mouse during sinus rhythm ($r^2 = 0.35$, $P = 0.16$).

ECG did not reflect genetically induced changes in repolarizing ion channel function (47). Parenthetically, we are not suggesting that the terminology of *b* and *c* waves replace standard electrocardiography designation of ventricular depolarization and repolarization. These terms were used only for convenient identification of these deflections in this study.

The variability in designation of the T wave described above also raises the question of the effects of anesthesia and whether it is responsible for the discrepancies because different anesthetics may have different effects on heart electrical activity. ECGs have been recorded in the absence of anesthesia (32, 33, 37) or using anesthesia with ketamine and xylazine (2, 16, 21), ketamine and pentobarbital sodium (5, 6, 29), ketamine and narcotic (22), halothane (4), ether (38), diazepam (29), and pentobarbital sodium (this study, and Refs. 31 and 32). It is not obvious from these studies whether or not the appearance of the different waves is anesthetic dependent. We could find no description of the effects of pentobarbital sodium, the anesthetic that we used, as well as other anesthetics, on the murine action potential.

We recorded 12-lead ECGs in the anesthetized mouse with the chest closed. Under these conditions, the largest deflection (*a* wave) almost always terminated in a second lower amplitude deflection (*b* wave), as previously described. The slow terminal wave (*c* wave) was infrequently recognized. Therefore, this wave, if representing ventricular repolarization (see below), could not be reliably recorded on the ECG. When the chest was opened in our experiments (and

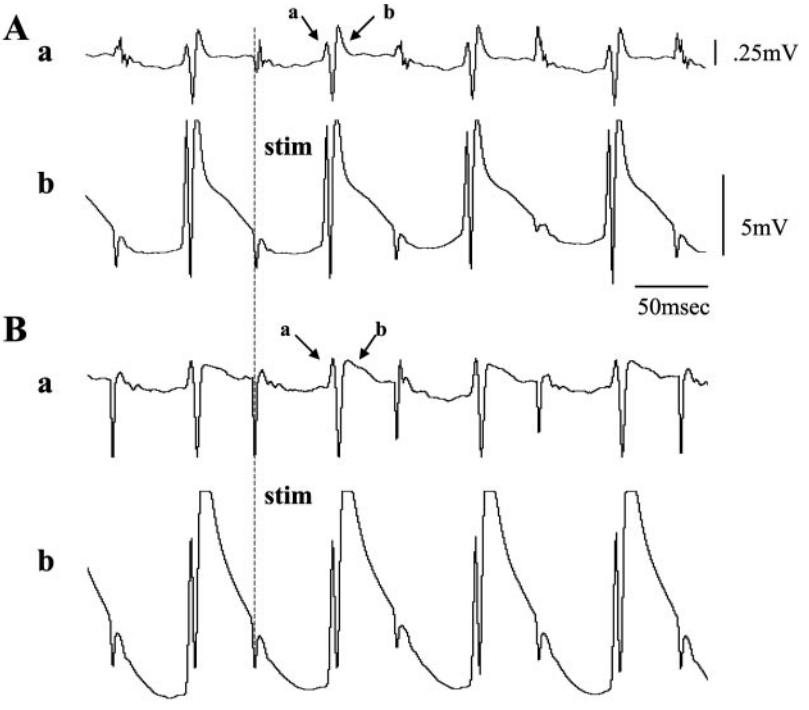

Fig. 8. Effects of 4-aminopyridine (4-AP) during atrial pacing at a SCL of 100 ms on ECG lead II (*top trace*) and MAP (*bottom trace*). Vertical dashed line shows atrial stimulus (stim) artifact. *A*: control values are the following: Qa = 8 ± 0, Qb = 25 ± 1, APD_{50} = 16 ± 1, APD_{90} = 54 ± 2. *B*: after 4-AP; Qa = 8 ± 0 ms, Qb = 44 ± 1 ms, APD_{50} = 30 ± 1 ms, APD_{90} = 63 ± 1 ms.

Table 5. *Effects of 4-AP on ECG and MAP*

		Control						4-AP				
Experiment	SCL	Qa	Qb	APD_{50}	APD_{90}	VERP	SCL	Qa	Qb	APD_{50}	APD_{90}	VERP
					Atrial pacing							
6		10 ± 0	25 ± 1	13 ± 1	46 ± 1	36 ± 0		11 ± 1	38 ± 1	25 ± 1	63 ± 1	50 ± 0
7		10 ± 1	25 ± 2	13 ± 1	45 ± 1	32 ± 0						48 ± 0
8		13 ± 1	27 ± 0	17 ± 1	52 ± 1	33 ± 1		13 ± 1	35 ± 1	29 ± 1	61 ± 1	46 ± 0
9		8 ± 0	25 ± 1	16 ± 1	54 ± 2	37 ± 1		8 ± 0	44 ± 1	30 ± 1	63 ± 1	45 ± 0
10		7 ± 0	20 ± 0	14 ± 2	47 ± 1	29 ± 1		7 ± 0	40 ± 0	34 ± 2	62 ± 1	57 ± 4
11		7 ± 1	23 ± 1	15 ± 1	44 ± 1	29 ± 2		8 ± 1	31 ± 1	24 ± 1	51 ± 1	52 ± 3
12		8 ± 1	20 ± 1	16 ± 1	43 ± 1	28 ± 0		8 ± 1		32 ± 1	62 ± 1	52 ± 0
13		7 ± 1	21 ± 1	21 ± 1	50 ± 1	29 ± 1		8 ± 1	29 ± 1	25 ± 1	57 ± 1	48 ± 0
Means ± SE		9 ± 2	23 ± 3	16 ± 3	48 ± 4	32 ± 4		9 ± 2	36 ± 6	28 ± 4	60 ± 4	56 ± 4

		Control						4-AP				
Experiment	SCL	Qa	Qb	Qc	APD_{50}	APD_{90}	SCL	Qa	Qb	Qc	APD_{50}	APD_{90}
					Sinus rhythm							
8	113 ± 1	12 ± 0	24 ± 0	47 ± 3	20 ± 0	47 ± 1	120 ± 1	12 ± 0	33 ± 1	ND	28 ± 1	56 ± 1
10	115 ± 1	7 ± 1	20 ± 1	53 ± 4	16 ± 1	46 ± 1	125 ± 1	7 ± 0	38 ± 4	ND	24 ± 2	60 ± 4
11	106 ± 8	8 ± 0	21 ± 2	58 ± 4	12 ± 1	44 ± 3	131 ± 3	8 ± 0	30 ± 2	ND	23 ± 2	52 ± 3
Means ± SE	111 ± 5	9 ± 3	22 ± 2	53 ± 6	16 ± 4	46 ± 2	125 ± 6	9 ± 3	34 ± 4	ND	25 ± 3	56 ± 4

4-AP, 4-aminopyridine.

the MAP electrode placed on the ventricles), the slow third (*c*) wave could be identified in most hearts but not in all leads. These procedures may have induced changes in the position of the heart relative to the ECG leads, allowing the *c* wave to be seen. The *a* and *b* waves were not altered.

Murine MAP and its relationship to ECG. To address the issue of how repolarization of the ventricles is manifested on the murine ECG, we recorded ventricular MAPs with an electrode exerting slight pressure on the myocardium of the in vivo murine heart, as described by Franz et al. (15, 27). It has been well established that there is a close correlation between the time course of the MAP and the transmembrane action potential (10, 12–15, 19, 35, 41, 42). Repolarization in MAP recordings corresponds to the T wave of the ECG in larger mammals (15, 36, 42). Although we did not correlate MAP recordings from murine ventricles with transmembrane recordings, in a report (27), in which this has been done in the isolated heart, it has been shown that the MAP accurately depicts repolarization if electrode diameter is not >0.25 mm.

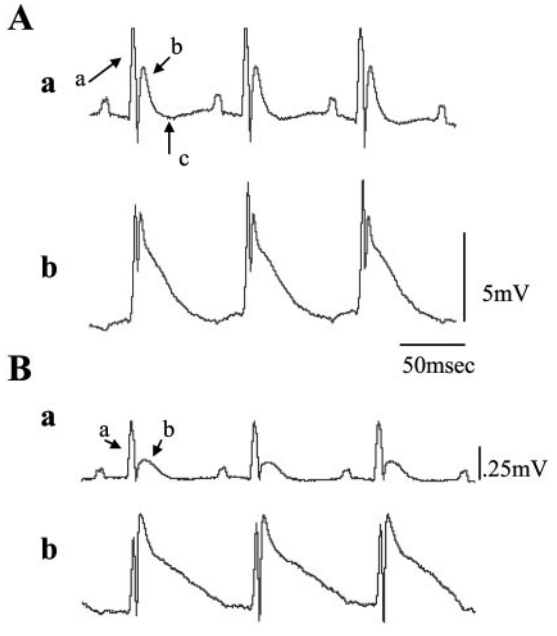

Fig. 9. Effects of 4-AP on ECG (lead I) and MAP during sinus rhythm. *a*, *b*, and *c* waves can be identified in control (*A*). After 4-AP (*B*), SCL is increased as is Qb, whereas the *c* wave has disappeared.

The contour of the MAPs resembled the murine ventricular transmembrane action potential, having an early rapid repolarization phase, and a slow terminal phase. At an average sinus cycle length of 113 ± 11 ms, the APD_{50} was 21 ± 6 ms, and APD_{90} was 53 ± 6 ms. Refractory period measurements mirrored the time course of repolarization on the MAP with the end of the effective refractory period occurring before complete repolarization (27). Measurements of APD_{50} of murine transmembrane action potentials have ranged from 3 to 25 ms (2, 8, 9, 11, 18, 21, 23, 24, 28, 32, 46, 48, 50) and APD_{90} or APD_{95} from 8 to 94.1 ms (2–4, 9, 11, 18, 21, 23, 24, 28, 32, 46, 48, 50). Thus our values are toward the high end of this range. They are also in agreement with some of the other studies where MAPs were measured in mice (22, 47). Our APD_{90} value is similar to that recently reported by Knollman et al. (27) in a study that directly compared MAPs with transmembrane potentials, but our APD_{50} is longer because of a small difference in the level at which phase 2 of the action potential begins; in our study it began at a slightly more positive level. Much of the transmembrane data comes from studies on single cells and the MAP data from isolated hearts (27), and therefore, a direct comparison with the in situ ventricles may not be warranted. The heart in situ is under the influence of many factors

(neurohumors, hormones, electrolytes, etc.) not always present in in vitro studies. In addition, our measurements are from epicardial muscle, whereas other measurements are from a variety of regions where action potential duration may differ (27).

From our data, it appears that the *a* wave and Qa interval on the ECG represent at least part of ventricular depolarization because they occur during the upstroke of the MAP. The *b* wave and the Qb interval occurred during repolarization of the MAP but did not account for complete repolarization because the Qb interval (22 ± 1 ms) was on average less than one-half the APD_{90} of the MAP (53 ± 6 ms). Richards et al. (38) proposed that repolarization may start before depolarization has ended in the murine heart and, therefore, the *b* wave may represent a terminal portion of ventricular depolarization that is fused with the beginning of repolarization. Studies (25, 26, 43) in mice in which ventricular conduction delay has been experimentally induced have found changes to occur primarily in the *a* wave, questioning whether the *b* wave is caused by the depolarizing wave front, and supporting the supposition that it reflects, at least in part, repolarization.

The average Qc interval that we measured while recording the MAP was 52 ± 5 ms while the APD_{90} of the MAP was 53 ± 6 ms ($P = 0.332$). On analysis by linear regression, there was no significant correlation between the Qc interval and the APD_{90} in individual experiments. The similar values of the Qc interval and APD_{90} nevertheless raise the suspicion that the *c* wave is involved in ventricular repolarization and the Qc interval represents complete repolarization. In several other studies, there was also a lack of correlation between QT interval and repolarization of the MAP or transmembrane potential (22, 28).

Why is there an absence of a well-defined QT interval in the murine heart? The shape of the ventricular transmembrane potential and MAP suggest a reason (27). The time course of repolarization lacks a plateau phase that separates depolarization (QRS) from repolarization (T) as in other mammalian hearts. In addition, the slow gradual time course for repolarization is expected to generate only weak electrical forces that may be responsible for the very low amplitude *c* wave when detectable.

Effects of 4-AP. To determine whether the *b* and/or *c* wave represents ventricular repolarization, we administered 4-AP, a chemical that blocks I_{to}, a major determinant of murine ventricular repolarization (11). 4-AP did not affect the Qa interval on the ECG, confirming that it represents ventricular depolarization, but it prolonged the Qb interval and the APD_{50} and APD_{90} of the MAP. VERP also lengthened. Therefore, we conclude that the *b* wave does reflect at least part of the time course of ventricular repolarization. However, given the greater duration of the APD_{90} (see above), repolarization as manifested on the surface ECG continues after the termination of the *b* wave. The effects of 4-AP on the *c* wave could not be ascertained during atrial pacing at rates fast enough to capture the rhythm of the heart because the pacing artifact and paced P waves obscured the location of a potential *c* wave. We were able to examine the effects of 4-AP on the *c* wave and Qc interval that were present during sinus rhythm, although 4-AP slows the heart rate. That the *c* wave disappeared in these experiments suggests that it was influenced by 4-AP and is involved in ventricular repolarization. Slowing of repolarization to a different extent in different regions of the ventricles may have reduced this deflection to such a low level that we were not able to detect it.

In conclusion, although it appears that both the *b* and *c* waves represent ventricular repolarization, neither the Qb nor the Qc intervals (when present) correlates exactly with APD_{90} of the MAP, an objective measure of ventricular repolarization. Furthermore, our study shows that the third deflection (*c* wave) is not reliably identifiable (1, 22, 30, 31, 37, 38, 47). As discussed above, well-defined T wave and QT interval may be absent because of the voltage time course of the ventricular transmembrane potential. Therefore, an accurate measurement of complete repolarization of the murine ventricle cannot usually be obtained from the surface ECG.

This study was supported by National Heart, Lung, and Blood Institute Grant HL-30557. C. Cabo was supported in part by a research grant from The Whitaker Foundation.

REFERENCES

1. **Agduhr E and Stenstrom N.** The appearance of the electrocardiogram in heart lesions produced by cod liver oil treatment. *Acta Paediatr* 33: 493–588, 1929.
2. **Babij P, Roger-Askew G, Nieuwenhuijsen B, Su CM, Bridal TR, Jow B, Argentieri TM, Kulik J, DeGennero LJ, Spinelli W, and Colatski TJ.** Inhibition of cardiac delayed rectifier K^+ current by overexpression of the long QT-syndrome HERG G628S mutation in transgenic mice. *Circ Res* 83: 668–678, 1998.
3. **Baker LC, London B, Choi BR, Koren G, and Salama G.** Enhanced dispersion of repolarization and refractoriness in transgenic mouse hearts promotes reentrant ventricular tachycardia. *Circ Res* 86: 396–407, 2000.
4. **Barry D, Xu H, and Schuessler RB.** Functional knockout of the transient outward current, long QT syndrome, and cardiac remodeling in mice expressing a dominant-negative Kv4 alpha subunit. *Circ Res* 83: 560–567, 1998.
5. **Berul C, Christie M, Aronovitz M, Seidman CE, Seidman JG, and Mendelsohn ME.** Electrophysiological abnormalities and arrhythmias in alpha MHC mutant familial hypertrophic cardiomyopathy mice. *J Clin Invest* 99: 570–576, 1997.
6. **Berul CI, Aronovitz MJ, and Wang PJ.** In vivo cardiac electrophysiology studies in the mouse. *Circulation* 94: 2641–2648, 1996.
7. **Bevilaqua LM, Maguire CT, Seidman JG, Seidman CE, and Berul CI.** QT dispersion in alpha myosin heavy-chain familian hypertrophic cardiomyopathic mice. *Pediatr Res* 45: 643–647, 1999.
8. **Binah O, Arieli R, Beck R, Rosen MR, and Palti Y.** Ventricular electrophysiological properties: is interspecies variability related to thyroid state? *Am J Physiol Heart Circ Physiol* 252: H1265–H1274, 1987.
9. **Charpentier F, Merot J, Riochet D, Le Marec H, and Escande D.** Adult KCNE1-knockout mice exhibit a mild cardiac cellular phenotype. *Biochem Biophys Res Commun* 251: 806–810, 1998.
10. **Dean J and Lab M.** Effect of changes in load on monophasic action potential and segment length of pig heart in situ. *Cardiovasc Res* 23: 887–896, 1989.

11. **Dubell WH, Lederer WJ, and Rogers TB.** K^+ currents responsible for repolarization in mouse ventricle and their modulation by FK-506 and rapamycin. *Am J Physiol Heart Circ Physiol* 278: H886–H897, 2000.
12. **Franz M, Bargheer K, Rafflenbeurl W, Haverich A, and Lichtlen PR.** Monophasic action potential mapping in human subjects with normal electrocardiograms: direct evidence for the genesis of the T wave. *Circulation* 75: 379–386, 1987.
13. **Franz MR, Burkhoff D, Spurgeon H, Weisfeldt ML, and Lakatta EG.** In vitro validation of a new cardiac catheter technique for recording monophasic action potentials. *Eur Heart J* 7: 34–41, 1986.
14. **Franz MR.** Long term recording of monophasic action potentials form human endocardium. *Am J Cardiol* 51: 1629–1634, 1983.
15. **Franz MR.** Method and theory of monophasic action potential recording. *Prog Cardiovasc Dis* 33: 347–368, 1991.
16. **Gloss B, Sayen MR, Trost SU, Bluhm WF, Meyer M, Swanson EA, Usala SJ, and Dillmann WH.** Altered cardiac phenotype in transgenic mice carrying the 337 threonien thyroid hormone receptor B mutant derived from the S family. *Endocrinology* 140: 897–902, 1999.
17. **Guo W, Li H, London B, and Nerbonne J.** Functional consequences of elimination of $i_{(to,f)}$ and $i_{(to,s)}$: early afterdepolarizations, atrioventricular block, and ventricular arrhythmias in mice lacking Kv1.4 and expressing a dominant-negative Kv4 alpha subunit. *Circ Res* 87: 73–79, 2000.
18. **Heath BM, Xia J, Dong E, An RH, Brooks A, Liang C, Federoff HJ, and Kass RS.** Overexpression of nerve growth factor in the heart alters ion channel activity and β adrenergic signaling in an adult transgenic mouse. *J Physiol* 512: 779–791, 1998.
19. **Hoffman BF, Cranefield PF, Lepeschkin E, Surawicz B, and Herrlich HC.** Comparison of cardiac monophasic action potentials recorded by intracellular and suction electrodes. *Am J Physiol* 196: 1297–1301, 1959.
20. **Huen D, Fox A, Kumar P, and Searle PF.** Dilated heart failure in transgenic mice expressing the Epstein-Barr virus nuclear antigen-leader protein. *J Clin Virology* 74: 1381–1391, 1993.
21. **Jeron A, Mitchell G, Zhou J, Murata M, London B, Buckett P, Wiviott SD, and Koren G.** Inducible polymorphic ventricular tachyarrhythmias in a transgenic mouse model with long Q-T phenotype. *Am J Physiol Heart Circ Physiol* 278: H1891–H1898, 2000.
22. **Johansson C, Vennstrom B, and Thoren P.** Evidence that decreased heart rate in thyroid hormone receptor-α1-deficient mice is an intrinsic defect. *Am J Physiol Regulatory Integrative Comp Physiol* 275: R640–R646, 1998.
23. **Johnson BD, Zheng W, Korach KS, Scheuer T, Catterall WA, and Rubanyi GM.** Increased expression of the cardiac L-type channel in estrogen receptor-deficient mice. *J Gen Physiol* 110: 135–140, 1997.
24. **Johnson CM, Green KG, Kanter EM, Bou-Abboud E, Saffitz JE, and Yamada KA.** Voltage-gated Na^+ channel activity and connexin expression in Cx43-deficient cardiac myocytes. *J Cardiovasc Electrophysiol* 10: 1390–1401, 1999.
25. **Kirchhoff S, Nelles E, Hagendorf A, Kruger O, Traub O, and Willecke K.** Reduced cardiac conduction velocity and predisposition to arrhythmias in connexin 40-deficient mice. *Curr Biol* 8: 299–302, 1998.
26. **Kishimoto C, Matsumori A, Ohmae M, Tomioka N, and Kawai C.** Electrocardiographic findings in experimental myocarditis DBA/2 mice: complete atrioventricular block in the acute stage, low voltage of the QRS complex in the subacute stage and arrhythmias in the chronic stage. *J Am Coll Cardiol* 3: 1461–1468, 1984.
27. **Knollman BC, Katchman AN, and Franz MR.** Monophasic action potential from intact mouse heart: validation, regional heterogeneity, and relation to refractoriness. *J Cardiovasc Electrophysiol* 12: 1286–1294, 2001.
28. **Knollmann BC, Knollmann-Rischel BEC, Weissmann NJ, Jones LR, and Morad M.** Remodelling of ionic currents in hypertrophied and failing hearts of transgenic mice overexpressing calsequestrin. *J Physiol* 525: 483–498, 2000.
29. **Kupershmidt S, Yang T, Anderson ME, Wessels A, Niswender KD, Magnuson MA, and Roden DM.** Replacement by homologous recombination of the *min K* gene with *lacZ* reveals restriction of *minK* expression to the mouse cardiac conduction system. *Circ Res* 84: 146–152, 1999.
30. **Lepeschkin E.** The configuration of the T wave and the ventricular action potential in different species of mammals. *Ann NY Acad Sci* 127: 170–178, 1965.
31. **Lombard E.** Electrocardiograms of small mammals. *Am J Physiol* 171: 189–193, 1952.
32. **London B, Jeron A, Zhou J, Buckett P, Han X, Mitchell GF, and Koren G.** Long QT and ventricular arrhythmias in transgenic mice expressing the N terminus and first transmembrane segment of a voltage-gated potassium channel. *Proc Natl Acad Sci USA* 95: 2926–2931, 1998.
33. **Mitchell G, Jeron A, and Koren G.** Measurement of heart rate and QT interval in the conscious mouse. *Am J Physiol Heart Circ Physiol* 274: H747–H751, 1998.
34. **Nagel A.** The electrocardiogram of European shrews. *Comp Biochem Physiol* 83A: 791–794, 1986.
35. **Olsson SB.** Right ventricular monophasic action potentials during regular rhythm. *Acta Med Scand* 191: 145–157, 1972.
36. **Platia EV, Weisfeldt ML, and Franz MR.** Immediate quantitation of antiarrhythmic drug effect by monophasic action potential recording in coronary artery disease. *Am J Cardiol* 61: 1284–1287, 1988.
37. **Rappaport M and Rappaport I.** Electrocardiographic considerations in small animal investigations. *Am Heart J* 26: 662–680, 1943.
38. **Richards AG, Simonson S, and Visscher MB.** Electrocardiogram and phonogram of adult and newborn mice in normal conditions and under the effect of cooling, hypoxia, and potassium. *Am J Physiol* 174: 293–298, 1953.
39. **Roden DM, Lazzara R, Rosen M, Schwartz PJ, Towbin J, and Vincent GM.** Multiple mechanisms in the long QT syndrome. *Circulation* 94: 1996–2012, 1996.
40. **Sambhi MP and White FN.** The electrocardiogram of the normal and hypertensive rat. *Circ Res* 8: 129–134, 1960.
41. **Seed WA, Noble M, Oldershaw P, Wanless RB, Drake-Holland AJ, Redwood D, Pugh S, and Mills C.** Relation of human cardiac action potential duration to the interval between beats: implications for the validity of the rate corrected QT interval (QTc). *Br Heart J* 57: 32–37, 1987.
42. **Stroobandt R, Brachmann J, Bourgeois I, Wielders P, Kubler W, and Senges J.** Simultaneous recording of atrial and ventricular monophasic action potentials: monophasic action potential duration during atrial pacing, ventricular pacing, and ventricular fibrillation. *Pacing Clin Electrophysiol* 8: 502–511, 1985.
43. **Verheule S, van Batenburg C, Coenjaerts F, Kirchhoff S, Willecke K, and Jongsma HJ.** Cardiac conduction abnormalities in mice lacking the gap junction protein connexin 40. *J Cardiovasc Electrophysiol* 10: 1380–1389, 1999.
44. **Vornanen M.** Basic functional properties of the cardiac muscle of the common shrew (sorex araneus) and some other small mammals. *J Exp Biol* 145: 339–351, 1989.
45. **Wang L and Duff HJ.** Developmental changes in transient outward current in mouse ventricle. *Circ Res* 81: 120–127, 1997.
46. **Wang L, Feng ZP, Kondo CS, Sheldon RS, and Duff HJ.** Developmental changes in the delayed rectifier K^+ channels in mouse heart. *Circ Res* 79: 79–85, 1996.
47. **Wickenden AD, Lee P, Sah R, Huang Q, Fishman GI, and Backx PH.** Targeted expression of a dominant-negative $Kv4.2K^+$ channel subunit in the mouse heart. *Circ Res* 85: 1067–1076, 1999.
48. **Xu H, Barry D, Huilin L, Brunet S, Guo W, and Nerbonne JM.** Attenuation of the slow component of delayed rectification, action potential prolongation, and triggered activity in mice expressing a dominant-negative Kv2 alpha subunit. *Circ Res* 85: 623–633, 1999.
49. **Zhou J, Jeron A, London B, Han H, and Koren G.** Characterization of a slowly inactivating outward current in adult mouse ventricular myocytes. *Circ Res* 83: 806–814, 1998.
50. **Zhou YY, Song LS, Lakatta EG, Xiao RP, and Cheng H.** Constitutive β_2 adrenergic signaling enhances sarcoplasmic reticulum calcium cycling to augment contraction in mouse heart. *J Physiol* 521: 351–361, 1999.